

Accounting for Deterministic Trends in Geostatistical Modeling of Categorical and Continuous Variables

C. V. Deutsch, Y. Xie, and Z. A. Reza, University of Alberta
(cdeutsch@civil.ualberta.ca, ylxie@civil.ualberta.ca, zreza@ualberta.ca)

B. Norris, Canadian Petroleum Ltd.
(brett_norris@cdnpet.com)

Abstract

The variability of regionalized variables consists partly of deterministic variation and partly of stochastic variation. In practice, lithofacies and petrophysical properties such as porosity and permeability are not entirely deterministic nor entirely stochastic. Deterministic variations are best modeled by an explicit trend model, that is, not left to chance. Stochastic variations are best modeled by geostatistical techniques, which account for the spatial correlation structure of the stochastic variation.

The separation of deterministic and stochastic variations must be done with care. Overfitting the deterministic component leads to reduced uncertainty and property models with too little heterogeneity. Not fitting deterministic aspects of property variation lead to property models that do not reproduce “real” geologic trends and thus to poor reservoir forecasts. This paper presents procedures and programs to (1) fit deterministic trends, (2) remove trends from data, and (3) introduce the trends back in after geostatistical modeling of the stochastic variations.

Categorical (lithofacies) and continuous (porosity and permeability) variables must be handled differently. It is possible to separate a continuous variable into a trend and stochastic residual, that is, $Z = m + R$; however, no such separation is possible with categorical variables. Prior deterministic proportion models must be considered in the stochastic modeling of categorical variables. The methodology, programs, and case study address both types.

KEYWORDS: facies modeling, petrophysical property modeling, reservoir forecasting, uncertainty analysis

Introduction

Increasing demand is being placed on numerical reservoir models to provide reliable predictions of reservoir performance. Alternative production scenarios, well locations, well trajectories, and infill opportunities are being compared and chosen with the assistance of flow simulation using numerical reservoir models. The efficacy of such numerical models can only be assured when they reproduce all relevant information including conceptual geologic trends.

Early reservoir models were entirely deterministic. These simplistic layer-cake models reproduced large scale geologic features, but did not capture small scale variations and heterogeneities that affect flow performance. Nevertheless, such 3-D numerical reservoir models were used with success for many years. The necessity of introducing realistic heterogeneity in reservoir models was driven by the desire for more accurate forecasts and more powerful software and computers, which require more detailed numerical models.

Geostatistical methods have gained popularity to more accurately reflect stochastic heterogeneity. The value of such geostatistical models is unquestioned. Nevertheless, a legitimate criticism of

geostatistical models is that they do not capture geologic features and patterns that are known to exist. A limited number of studies exist to show that such features have an affect on fluid flow predictions. Although we are not in the “business of creating pretty pictures (Journel, 1993) [6]” we aim to create numerical geologic models that have significant predictive ability. It is critical that such models reproduce all available information including geologic trends and patterns. Through application to real reservoir problems, an increasing number of practicing reservoir geoscientists and engineers are realizing this [1, 4, 5, 7].

Reverting to completely deterministic models would be a mistake. Our aim is to show that we can have the best of both worlds, that is, merge deterministic and stochastic models. For continuous variables, this amounts to decompose the variable into a prior mean and a stochastic residual:

$$Z(\mathbf{u}) = m(\mathbf{u}) + R(\mathbf{u}) \quad \forall \mathbf{u} \in A$$

where, by convention, Z is the original variable, m is the prior mean or trend, R is the residual, \mathbf{u} is the 3-D locations coordinate vector, and A is the stationary area being modeled. The specification of $m(\mathbf{u}), \mathbf{u} \in A$ is deterministic whilst R is modeled as a random variable possible correlated to m .

Some geostatisticians have attempted to model the local mean $m(\mathbf{u}), \mathbf{u} \in A$ with stochastic models using different parameters; however, this fails to capture all the geologic knowledge about trend and variability since such modeling is based solely on the data at hand. Using the m as a locally varying mean in simple kriging applications (Deutsch and Journel, 1997 [2]) also fails to capture all of the information in m ; the weight to m is an artifact of data spacing.

The 3-D grid $m(\mathbf{u}), \mathbf{u} \in A$ should be modeled with significant expert intervention. Some fitting and gridding software could be used, but the emphasis should be on reflecting large-scale geologic features that are known to exist by consideration of (1) the data at hand, (2) a regional geologic interpretation, and (3) experience with analog reservoirs, outcrops, and modern depositional systems. As a practical detail, it is straightforward to model a 1-D vector of vertical variations and a 2-D vector of areal variations. These must be combined to a full 3-D trend model specification discussed later.

A different approach must be adopted for categorical variables, since there is no real “numerical” value to lithofacies types that would permit a separation into $Z = m + R$. Consider $k = 1, \dots, K$ mutually exclusive and exhaustive lithofacies types with global proportions $p_k, k = 1, \dots, K$. Specification of deterministic prior means takes the form of prior probabilities (or proportions):

$$p_k(\mathbf{u}), \quad k = 1, \dots, K, \forall \mathbf{u} \in A$$

where, $p_k(\mathbf{u})$ is between 0 and 1. Any departure from the global proportion p_k implies additional knowledge in the trend model. The prior mean values $p_k(\mathbf{u}), k = 1, \dots, K, \forall \mathbf{u} \in A$ are modeled by expert fitting as are the local mean values $m(\mathbf{u}), \mathbf{u} \in A$. We have the constraints that $p_k(\mathbf{u})$ be between 0 and 1 and $\sum_{k=1}^K p_k(\mathbf{u}) = 1.0$; however, the same basic procedures as used for continuous variables are followed. The lithofacies must be modeled using the prior mean values; it is not possible to separate the mean and residual and perform separate modeling. This will be discussed.

Methodology

Reservoir models can be improved by consideration of deterministic trends. The most important question is how much variation to put into the trend and how much to leave to stochastic modeling. This question amounts to the “decision of stationarity,” which has led to much controversy and misunderstanding over the years. Perhaps the most important step in geostatistics is ensuring that the variable being modeled is stationary over the study area. Geologic modelers typically adopt one of two attitudes toward stationarity: (1) any decision of stationarity is unacceptable because the variation patterns are too complex for stochastic modeling, or (2) group the data by

Facies 1	V shale ≤ 0.11
Facies 2	$0.11 < \text{V shale} < 0.27$
Facies 3	V shale ≥ 0.27

Table 1: The definition of facies based on Vshale value

major stratigraphic layer and lithofacies and let local variation patterns be controlled by the data themselves. Both views have validity, but may be too extreme. There are complex patterns of variation that are important and yet the data must be grouped together somehow to proceed with any numerical modeling.

Clearly, we should not overdo trend modeling. Our understanding of the mean $m(\mathbf{u})$ changes with the amount of data we have and can be made more precise with more extensive data. The scale of the mean variations we consider should be significantly larger than the data spacing and be backed up by geological interpretation. Explicit accounting of variations at smaller scale is unjustified. Cross validation may be of assistance in determining the correct decomposition of the grades into mean and residual.

Case Study

Lithofacies, porosity, and permeability data from a reservoir interval in a field in Yemen are considered. There was clear evidence of geological trends in these three variables.

This study focuses on a thin reservoir layer with production potential. A global trend is apparent in the gross thickness of the layer that dips southeasterly. Also, there is a significant trend in NTG (net-to-gross) ratio in the southward direction. Explicit estimation of the trends was considered.

The study is based on data from 46 wells. Well data of the entire region are used to capture global trends within the study area. There are 138 well data in the region. Figure 1 shows the locations of the 46 wells with their thickness indicated. We will simulate a 21 by 17 km² domain.

The facies type is derived from the Vshale values as defined in Table 1.

Figure 2 shows the distributions of V shale, porosity and permeability over all the wells. Distributions of porosity and permeability of both sand facies in the well data are shown in Figure 3. The spikes in the histograms are due to the assigned minimum values to high shale content. There is a strong correlation between porosity and permeability as shown in Figure 4. The correlation coefficient is 0.60 and the rank correlation coefficient is 0.88. The global proportions are 0.52 for facies 1, 0.25 for facies 2 and 0.24 for facies 3.

In order to follow the stratigraphy, a vertical transformation to stratigraphic coordinates is performed. The existing base z_b and top z_t of the stratigraphic layer are used to guide the transformation:

$$z' = \frac{z - z_b}{z_t - z_b} \bar{z}$$

and

$$\bar{z} = \frac{\sum_{i=1}^I (z_t^i - z_b^i)}{I}$$

where z is the depth of the original thickness depth coordinate system, \bar{z} is the average thickness of all I wells and z' is the stratigraphic vertical coordinate.

This coordinate transformation is reversible. When the simulation is done, the model will be back transformed by:

$$z = z_b + \frac{z'}{\bar{z}} \times (z_t - z_b)$$

Our procedure will be to establish stratigraphic structure, facies model, then porosity and permeability model for each facies separately. The porosity and permeability models will be merged into the facies model to get the final model. Figure 5 shows the procedure of this data processing step.

Stratigraphic Structure Modeling: Thickness Modeling

The top surface of the entire field is available together with the thickness of the stratigraphic layer at wells only. Thus, kriging and stochastic simulation were used to estimate the thickness for the simulation domain. Once the thickness (i.e., the top and bottom surfaces) values are obtained for the entire simulation volume, the stratigraphic coordinate transformation described above is executed and the simulation will be performed in regular Cartesian space. The simulated results will be transformed back into stratigraphic structure based on the top and the estimated base surface.

It is observed from all wells that there is a systematic trend in the thickness of the stratigraphic layer. From North to South, the thickness is continuously decreasing. From West to East, it remains constant and then decreases. Before we model the thickness of the simulation domain, we will explicitly account for this trend. The procedure:

- model the deterministic trend of the thickness explicitly,
- subtract the trend from well thickness data to compute the thickness residuals, which will be used as conditional data,
- model the residuals of the thickness by conditional sequential Gaussian simulation [3], and
- add the deterministic trend back to the simulated thickness residual to get a thickness model. This thickness model honors the thickness at wells.

The trends can be mathematically described as:

$$\text{North/South} \quad T = 10 + (Y - 169500) \times \frac{26}{70000}$$

$$\text{West/East} \quad T = T - (X - 295000) \times \frac{T-10}{2500}, \quad \text{if } X > 295000$$

Three Fortran programs are designed for handling this thickness trend. Program `trend01.for` calculates the thickness trend for the simulation grids using above equations, while `trend02.for` subtracts the trend from well thickness data to determine the thickness residuals which are used as conditional data in kriging and simulation for the entire simulation domain. Program `trend03.for` adds back the deterministic trend to simulated thickness residuals to obtain the final thickness model. Figure 6 shows the contour map of the thickness trend model.

Figure 7 shows the experimental variograms and variogram models of thickness residual. The variogram model and the thickness residual from the wells are used in the kriging and simulation of the thickness residual in the simulation grids. Thickness trend is added back to the estimated thickness residual to get the thickness model. Figures 8 and 9 show the kriged and simulated thickness residual and the thickness model, respectively.

Trend Modeling

Facies Trend Modeling

To establish the vertical trend in the stratigraphic transformed coordinate system, the wells are vertically split into 16 cells which is the number of vertical grids to be used for simulation. The number of data fallen into each cell is counted and the proportion of facies in the cell calculated.

For the areal trend, the wells in different regions of the entire area are grouped together and the average facies proportion in each region calculated. It is noticed that sand facies proportion decreases from North to South and from West to East at the same time.

Figure 10 shows the average vertical proportion of facies, which indicates trend much to the expectation of geologists: more of facies 3 is at the bottom (layer 16) where V-shale is higher. Figures 11 and 12 show the average facies proportions calculated from several control points along West- East and North-South directions and the trends are interpolated into the entire simulation interval along these two areal directions. Fortran program `d1interp.for` is designed for interpolating 1-D trend from few control points. From the three unidirectional trends, a 3-D trend model will be estimated in the form of local proportion curve of facies for each simulation grid cell.

Considering the natural order of sand facies and shale in this particular case, truncated Gaussian simulation will be used for the facies model. The transformation of facies code at wells into pseudo normal scores (conditional data for simulation) and the reverse transformation of the simulated normal scores into facies code (truncated) will be guided by the facies trend information, i.e., the local proportion curves (CDF) of facies in each simulated grid.

The 3-D facies proportion cube is not uniquely determined from the three 1-D proportion curves. We apply a sequential rescaling method to build the cube of facies proportions. Let PX_l ($PX_l^i, i = 1, \dots, I; l = 1, \dots, L$) denote the trend of facies proportion along West-East direction, PY_l ($PY_l^j, j = 1, \dots, J; l = 1, \dots, L$) denote the trend of facies proportion along North-South direction and PZ_l ($PZ_l^k, k = 1, \dots, K; l = 1, \dots, L$) denote the vertical trend of facies proportion, where L is the number of facies and I, J, K are the simulation dimensions.

The procedure to build the trend cube of facies proportion follows:

- The areal trend, PA_l , is obtained from the West-East and North-South trends. $PA_l = \frac{PX_l'}{\overline{PX_l}} \times PY_l$, where PX_l' denotes the transpose of PX_l and $\overline{PX_l}$ denotes the mean of trend vector, PX_l .
- Then, the areal trend will be populated for every slice along vertical direction to get the 3-D trend cube P_l . $P_l = PZ_l \otimes \frac{PA_l}{\overline{PA_l}}$. Once again, $\overline{PA_l}$ denotes the mean of the areal trend matrix, PA_l .
- This is repeated for all L facies to obtain $P_l, l = 1, \dots, L$.
- The proportion cubes are renormalized by making the summation of the proportion of all facies in the same grid cell equals to one: $P_l^{i,j,k} = \frac{P_l^{i,j,k}}{\sum_{l=1}^L P_l^{i,j,k}}, l = 1, \dots, L$.

Fortran program `d3prop.for` is used for the generation of 3-D trend cube of facies proportion. The program establishes 3-D local proportions from three 1-D trend curves based on the procedure described above. The 3-D local proportion of facies will be used in `GTSIM` [3] as an input to guide the truncation. The generated 3-D facies proportion trend is in the file `trend_cube.out`. Figure 13 shows the histogram of the facies proportion in the 3-D proportion cubes obtained.

Porosity and Permeability Trend Modeling

The trends in porosity and permeability have been determined in a similar way as the facies proportion trends. Figure 14 shows clear vertical trends of porosity in both sand facies. The average values of porosity along depth are shown as red dots in the plot. Based on geological information, interpreted are the trends (shown in green dots), which will be used in the trend modeling.

Areal trends have also been investigated. However, there is no clear indication of areal trend of porosity (see Figure 15). Hence, only vertical trends were considered for porosity.

Figures 16 and 17 show the vertical and areal average of permeability values, respectively. Figure 16 shows vertical trends in the average of permeability of both sand facies, which are similar

Facies 1	Facies 2
$T(x) = 3 - (X - 280000) \times \frac{0.3}{19000}$	$T(x) = 2.15 + (X - 280000) \times \frac{0.275}{25000}$
$T(y) = \begin{cases} 3.2 - \frac{1.0}{23000} \times (173500 - Y) & \text{if } Y \leq 1719000 \\ 2.54 & \text{otherwise} \end{cases}$	$T(y) = 2.15 - 4.94 \times (Y - 1722000)^2 \times 10^{-9}$

Table 2: The 1-D permeability trends for both facies 1 and 2

to that found in the porosity. Further, the strong correlation between porosity and permeability steers us to simulate porosity and permeability in a sequential manner, with the vertical trend to be accounted only once. This precludes the need for an explicit vertical trend model for permeability. However, there is an areal trend apparent in the permeability (see Figure 17). This areal trend will be modeled explicitly.

The areal trend in the permeability is captured using equations. Table 2 shows these equations for two 1-D trends in X and Y directions.

The final areal trend is calculated by taking the average of the two 1-D trends. Fortran program `g2dtrend.for` is designed to build 2-D trend explicitly based on two 1-D directions. The functions can be customized by subroutine `trendeqn.for`. Figure 18 shows the contour map of the areal trends of permeability for both facies 1 and 2.

The vertical trend of porosity and the areal trend of permeability will be removed from the porosity and permeability data from the wells, respectively. The residuals are used for further variography and simulation. Fortran program `gwltrend.for` computes the residuals of the well data for simulation. The same trend function subroutine as in `g2dtrend.for` are used.

Geostatistical Simulation

Figure 19 shows the experimental indicator variograms and variogram models for the three facies. The porosity and permeability residuals are transformed into the normal space. Variograms are computed on the transformed residual values, which will be used in the simulation. Variograms of porosity are shown in Figure 20 for both facies 1 and 2.

There is a natural transition in the facies (from sand facies 1 to sand facies 2 to shale) and there exists trends in the facies proportion both vertically and areally. Thus, facies modeling will be performed using truncated Gaussian simulation. The categorical facies data at wells are transformed into continuous Gaussian normal score values for conditioning data for sequential Gaussian simulation. The simulated continuous normal score variable is then truncated into facies types. The local facies proportion is required to guide the truncation. The local proportions are contained in the 3-D trend cubes of facies.

The categorical facies types must be transformed into continuous normal score values. The transformation is based on the facies proportion at the location of each well data. We use the middle value of the facies CDF as the representative value of that facies, that is,

$$cdf'_{i+1} = \begin{cases} \frac{cdf_i}{2} & i = 1 \\ \frac{cdf_i + cdf_{i+1}}{2} & i > 1 \end{cases}$$

Figure 21 illustrates such a transformation. In this specific situation, the facies proportions are: 50% of Facies 1, 25% of facies 2 and 25% of facies 3, and the corresponding CDF will be 0.50, 0.75 and 1, respectively. Based on the description above, the adjusted CDF will be: 0.25, 0.625 and 0.875. The corresponding normal score values are -0.6745, 0.3180 and 1.1503.

Fortran program `nscoref.for` is used to transform categorical facies type into pseudo normal score values. It needs both well data file and facies proportion (global or local in 3-D cube provided

by `d3prop.for`). The output will be the pseudo normal score of the well data.

Sequential Gaussian simulation [3] is used to generate normal score of facies type. The normal score of well data is used for conditioning. We require a single variogram model in normal space for SGSIM. For this purpose, the indicator variograms of each facies are calculated and modeled. Then indicator variograms will be transferred into normal variogram analytically as described by Deutsch [3]. Generally when indicator variograms are transformed into normal space, the variograms tends to be of Gaussian shape with shorter ranges. In this study, the indicator variogram of facies 1 is taken as representative for such transformation. Figure 22 shows the indicator variogram model of facies 1 and its corresponding normal score variogram model. 101 realizations were generated.

The facies type is obtained by truncating the simulated normal score values. The truncation is guided by local facies proportion available in the trend cube of facies proportions. Figure 23 illustrates the procedure of facies modeling.

The quality of the simulation can be verified by comparing the estimated facies type of the well data with the original well data, which can be done with GSLIB program `CHECKMOD` [3].

Figure 24 shows several plan views of the simulation volume. Figures 25 and 26 show several cross sections along North-South direction and West-East direction, respectively. These figures reveal similar trends of sand facies decreasing Southeasterly. The vertical trends are also captured in the simulated models.

Porosity and Permeability Modeling

The residuals of porosity and permeability are simulated for both facies 1 and 2 using SGSIM. The porosity and permeability models are obtained by adding the trend back on the simulated residuals. Figure 28 shows the histograms of the simulated porosity and permeability for both facies 1 and 2 from one realization.

Three general Fortran programs have been coded to facilitate the trend modeling. Program `g2dtrend.for` computes the trend values for a 2- D grid. The trend function can be externally edited with an external subroutine. Program `gwltrend.for` computes the residual values of well data required for conditioning in the simulation stage. It requires the same external subroutine for the trend equations as in `g2dtrend.for`. While `gretrend.for` adds back the trend to the simulated residual values to obtain the final models. This small code requires the output file from the simulation and the file with trend values in the simulated grid.

The 101 realizations facies models are ranked based on the proportion of net sand and three realizations, which are the 0.10, 0.50 and 0.90 quantile, are selected as representative of *low*, *base* and *high* facies models.

The simulated porosity and permeability models of facies 1 and facies 2 (facies 3 is shale and zeros are assigned) are applied to each of the facies model to get final porosity and permeability models.

Discussion

The stratigraphic structure of the field is simulated first. The facies, porosity and permeability models are estimated by modeling known existing trends (both vertical and areal) deterministically and the residual stochastically after trends taken away. Additional information based on the geology is considered in the model building process. The quality of the model will be evaluated by further flow simulation studies.

There are a number of approaches to integrate categorical and continuous random variables. This is true when dealing with variations that have both stochastic and deterministic nature. Decisions of “stationarity” are very important in devising methodologies for modeling.

Limitations and Future Work

No objective criterion has been developed to judge the appropriateness of the separation of deterministic and stochastic variations. It is unlikely that one could ever be determined. Nevertheless, additional study is warranted to provide some check that the separation is capturing valid geologic variations with a reasonable measure of uncertainty.

There is no unique approach to convert 1-D plus 2-D trend models to a 3-D trend cube. Additional testing and consideration of alternate methods would be worthwhile. The goal will be to reproduce the lower dimensional trend models while not introducing artifacts in the final 3-D models.

We encounter a paradox as more data becomes available. The additional data provide the means to identify a more reliable trend model, but they also make the trend model less important. That is, the conditioning of geostatistical models to many data enforces both the deterministic and stochastic variations of the variable of interest. Clearly, the usage of trend models is important in presence of sparse data. Additional work is warranted to provide guidelines on when trend models should be considered.

Conclusion

We have presented methods to model deterministic trends and then to ensure that geostatistical reservoir models reproduce those trends. This is very important in presence of sparse well control.

References

- [1] H. Beucher, A. Galli, G. Le Loc'h, and C. Ravenne. Including a regional trend in reservoir modelling using the truncated Gaussian method. In A. Soares, editor, *Geostatistics-Troia*, volume 1, pages 555–566. Kluwer, Dordrecht, Holland, 1993.
- [2] C. V. Deutsch and A. G. Journel. *GSLIB: Geostatistical Software Library and User's Guide*. Oxford University Press, New York, 1992.
- [3] C. V. Deutsch and A. G. Journel. *GSLIB: Geostatistical Software Library and User's Guide*. Oxford University Press, New York, 2nd edition, 1998.
- [4] P. Goovaerts. *Geostatistics for Natural Resources Evaluation*. Oxford University Press, New York, 1997.
- [5] E. H. Isaaks and R. M. Srivastava. *An Introduction to Applied Geostatistics*. Oxford University Press, New York, 1989.
- [6] A. G. Journel and J. J. Gómez-Hernández. Stochastic imaging of the Wilmington clastic sequence. *SPEFE*, pages 33–40, March 1993. SPE paper # 19857.
- [7] Y. Xie, A. S. Cullick, and C. V. Deutsch. Sediment trend models within subseismic stratigraphic surfaces for subsurface characterization. *SRC Memorandum*, in reproduction, 1999.

APPENDIX: Example Parameter files

Examples of the parameter files used in this study are shown in: Figures 29, 30, 31, 32, 33, 34, 35 and 36.

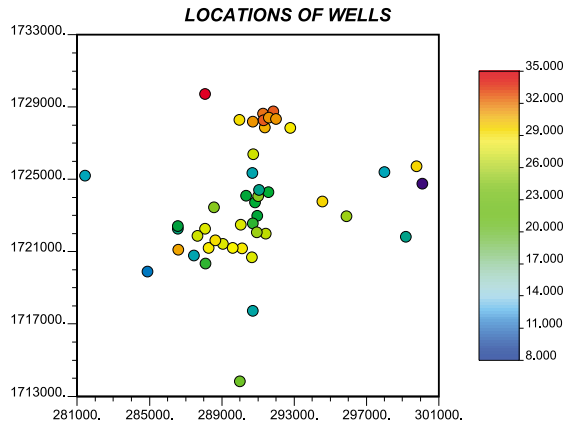


Figure 1: Well locations and their thickness.

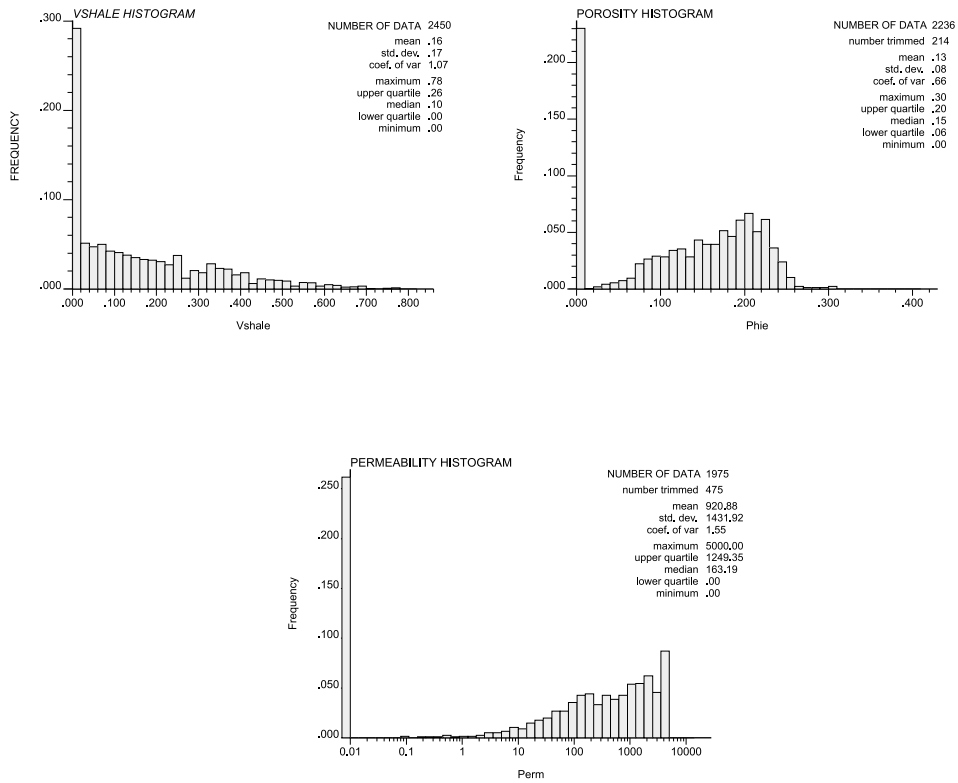


Figure 2: Histograms of Vshale, porosity and permeability.

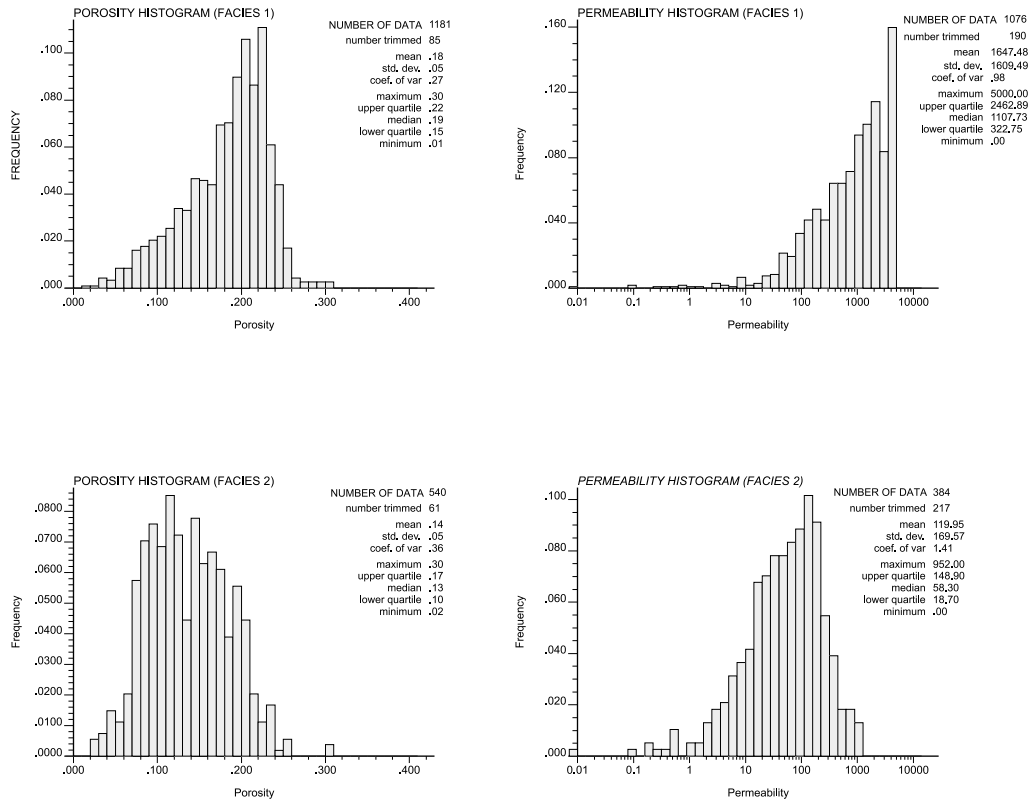


Figure 3: Histograms of porosity (left) and permeability (right) in facies 1 (top) and facies 2 (bottom).

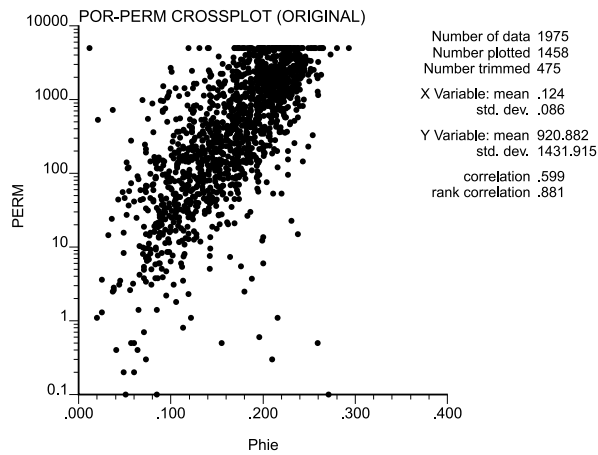


Figure 4: Cross plot of permeability versus porosity.

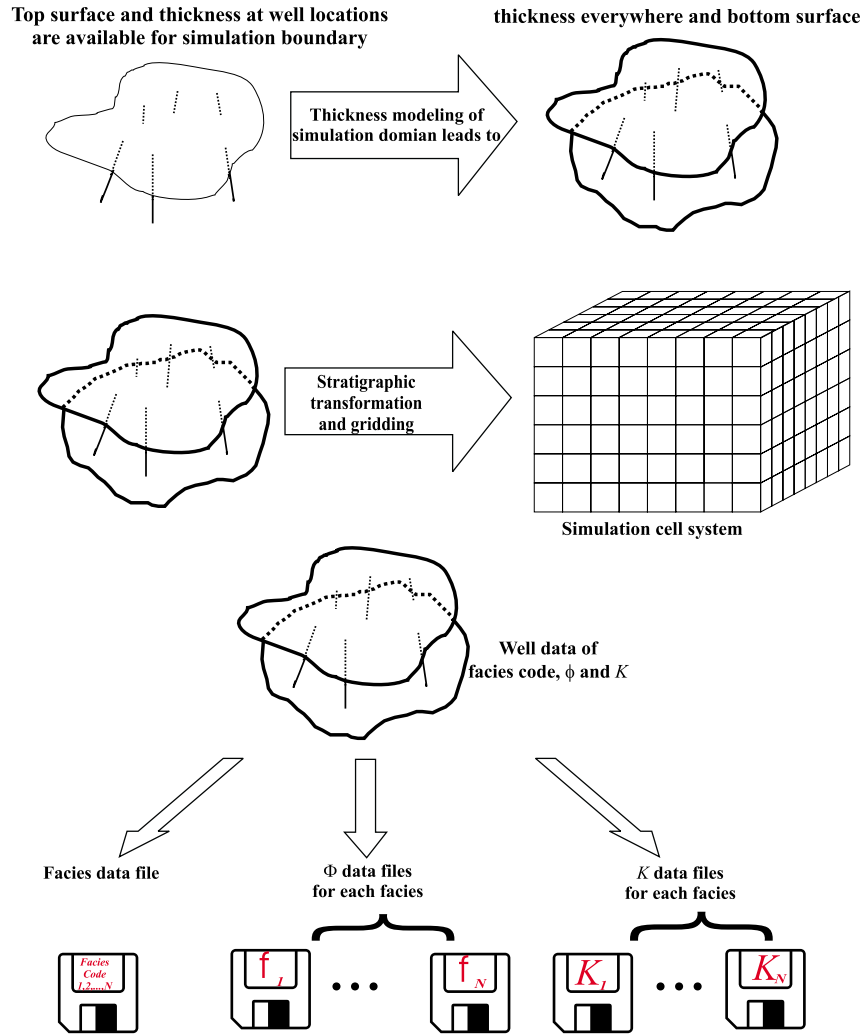


Figure 5: Scheme of data preprocessing.

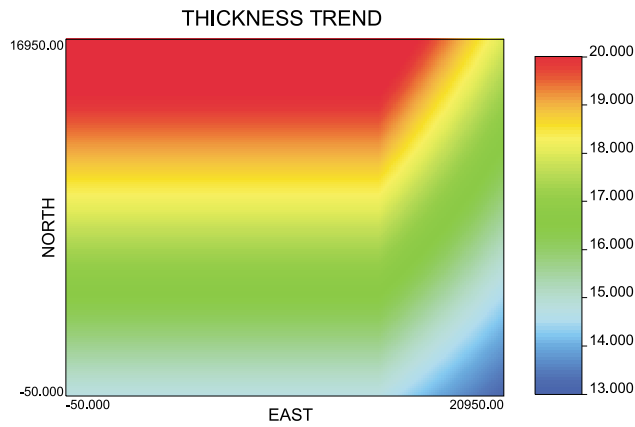


Figure 6: The contour map of the trend in the thickness.

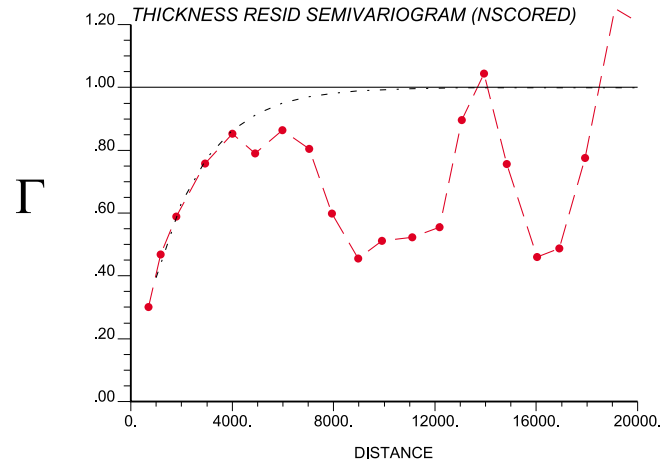


Figure 7: Variogram and variogram model of thickness residual.

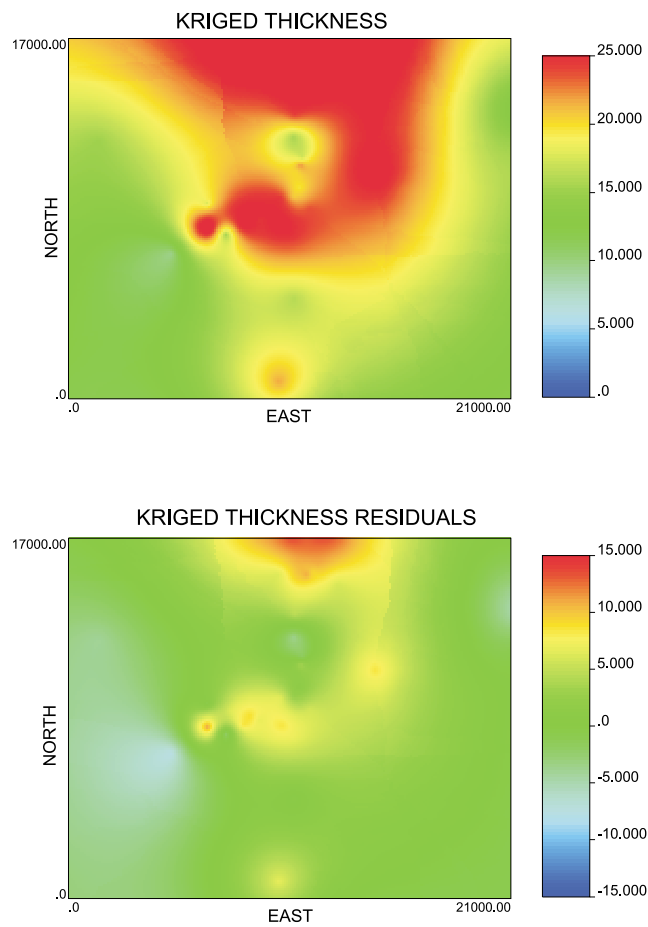


Figure 8: A realization of kriged thickness residual (bottom) and the thickness model after adding the trend (top).

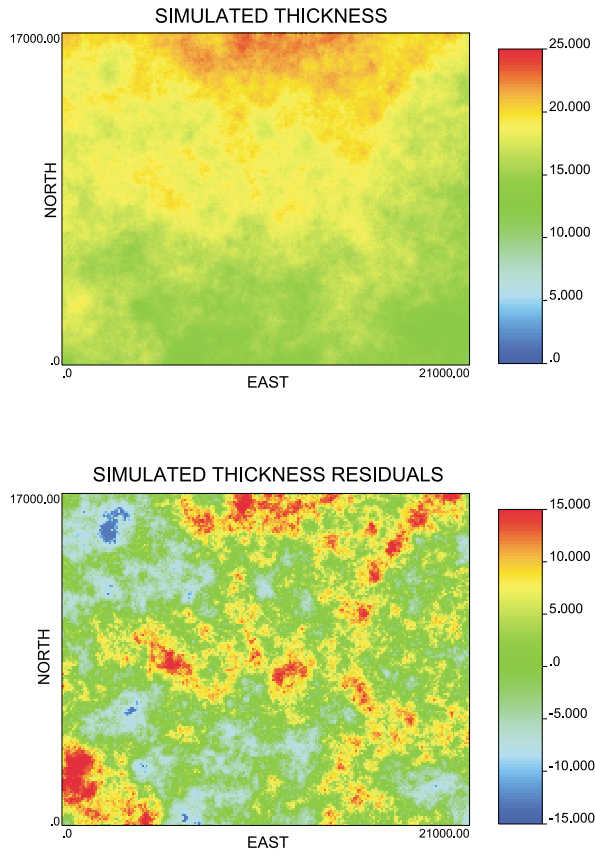


Figure 9: A realization of simulated thickness residual (bottom) and the thickness model after adding the trend (top).

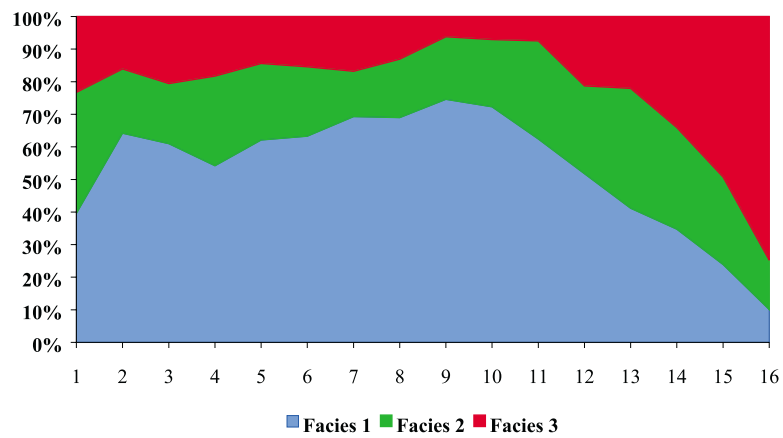


Figure 10: Vertical facies proportions. Layer 1 is at the top and layer 16 at the bottom.

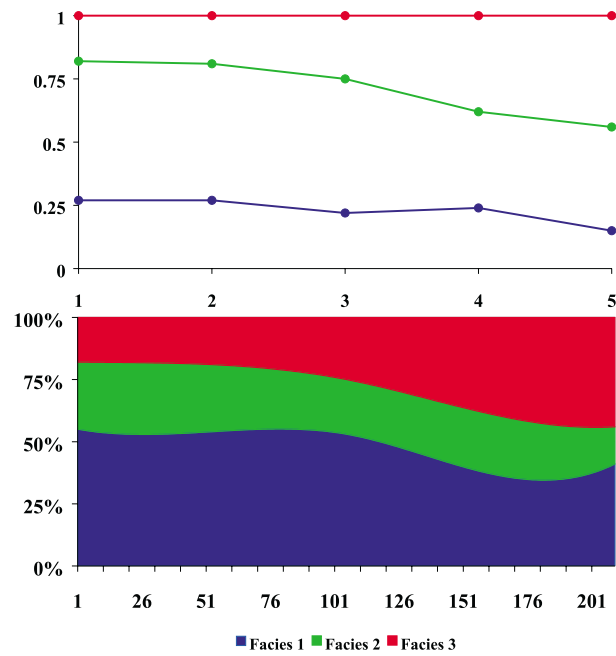


Figure 11: a) facies proportion along West-East direction at control points; b) interpolated facies proportions.

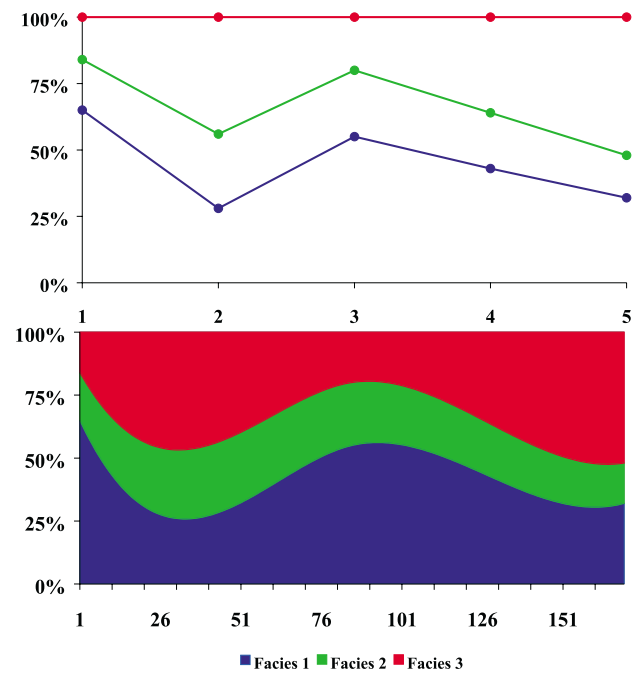


Figure 12: a) facies proportion along North-South direction at control points; b) interpolated facies proportions.

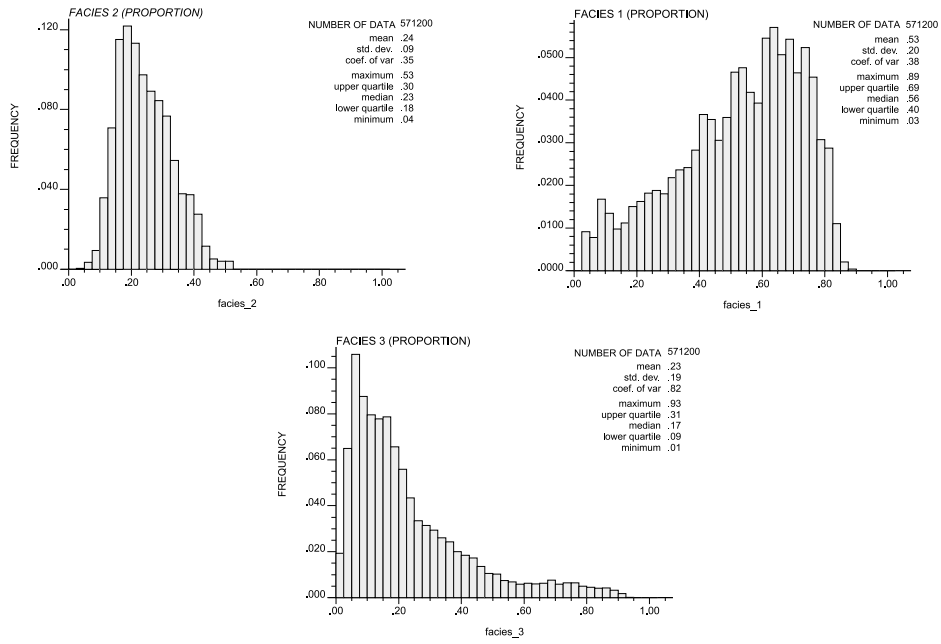


Figure 13: The histograms of three facies proportion in the 3-D proportion trend cubes.

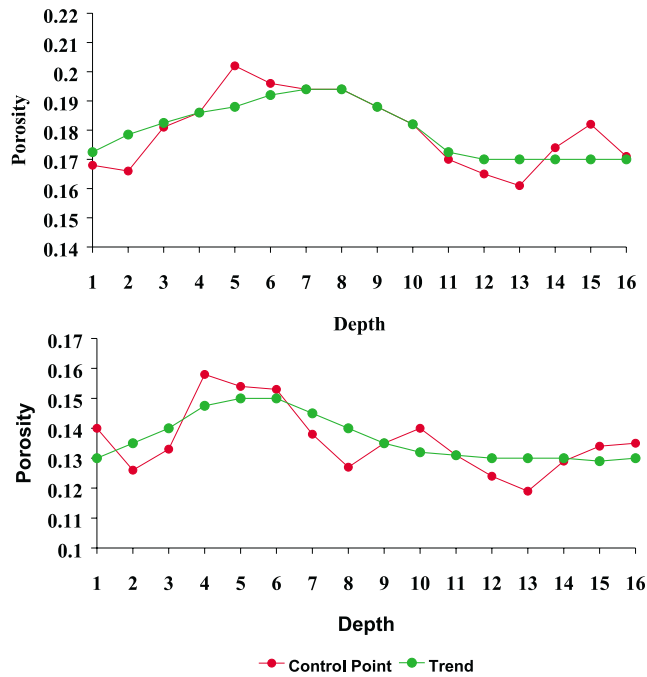


Figure 14: Vertical average (red dots: control points) and interpreted trends (green dots: interpreted trend) in porosity of facies 1(top) and facies 2(bottom).

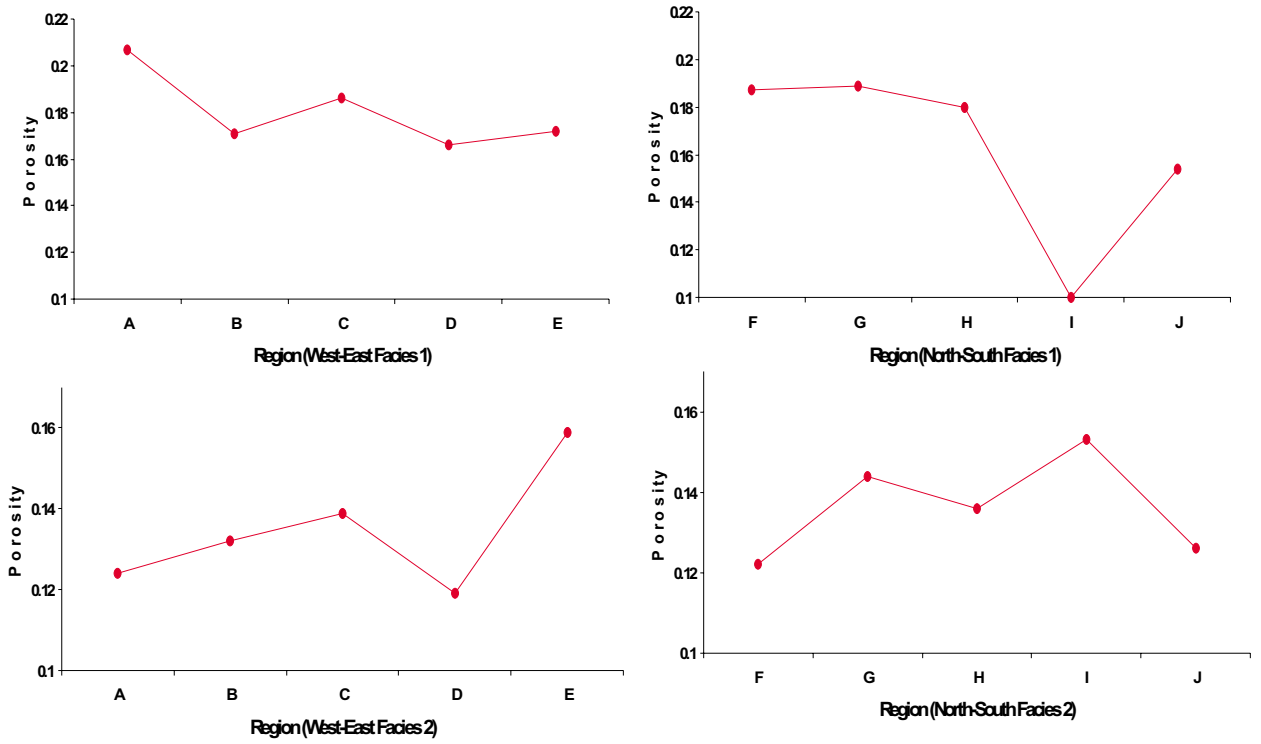


Figure 15: Average value of porosity of control regions; left: West-East direction; right: North-South direction; top: Facies 1; and bottom: Facies 2.

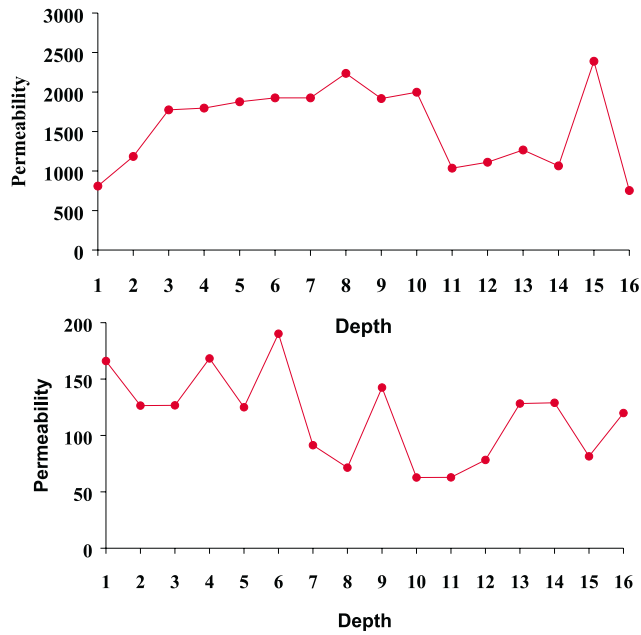


Figure 16: Vertical average in permeability of facies 1 (top) and facies 2 (bottom).

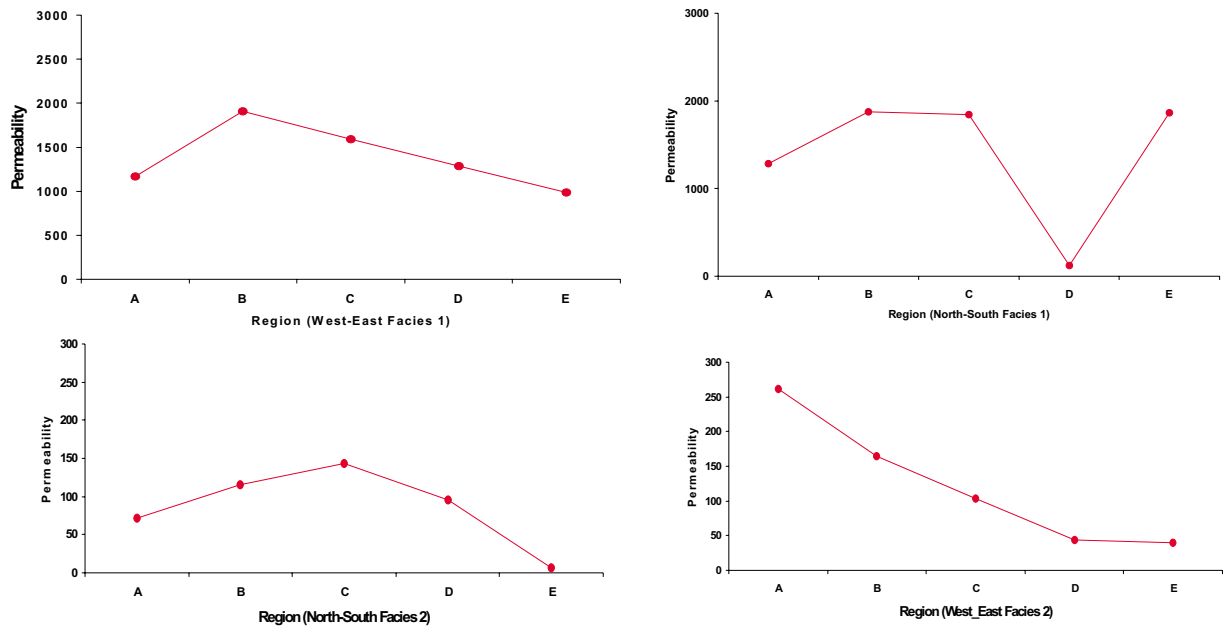


Figure 17: Average value of permeability of control regions; **left**: West-East direction; **right**: North-South direction; **top**: Facies 1; and **bottom**: Facies 2.

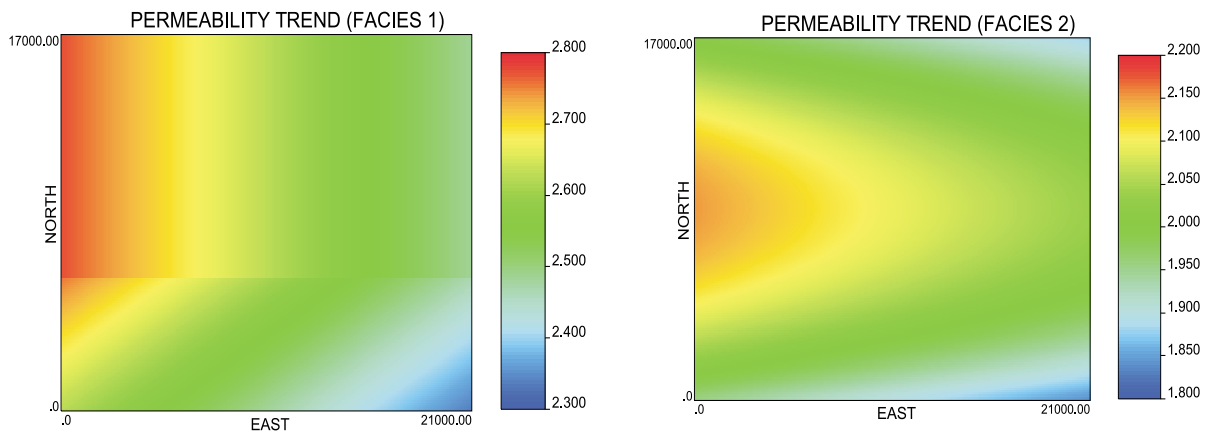


Figure 18: The contour map of permeability trends of facies 1 (top) and facies 2 (bottom).

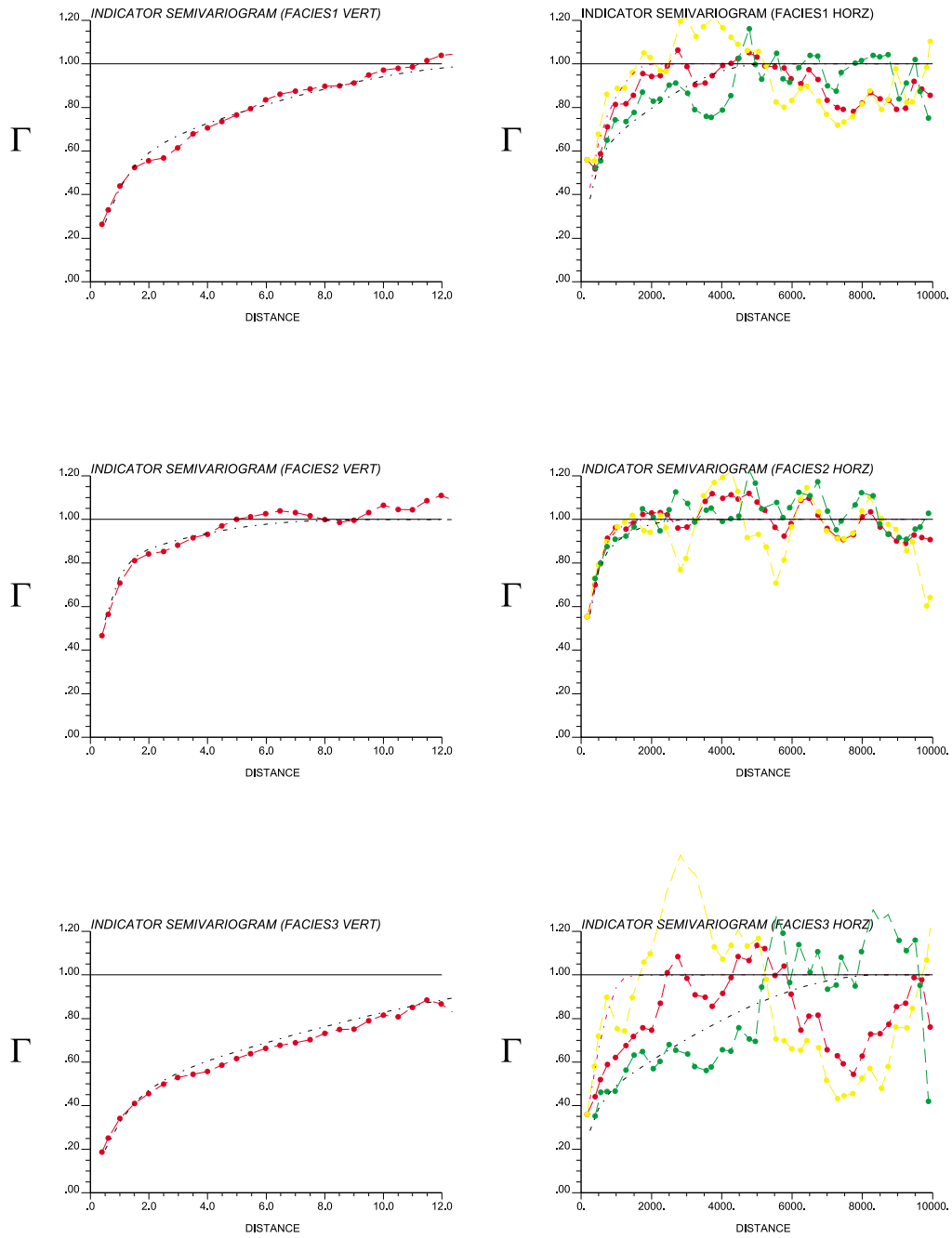


Figure 19: Experimental indicator variograms (dotted lines) and variogram models (dashed lines) for facies 1 (top), facies 2 (middle) and facies 3 (bottom). Yellow: northing; green: easting; red: omni-directional horizontal variogram.

Figure 20: Porosity residual variograms for facies 1 and 2 (same color scheme as in Figure 19).

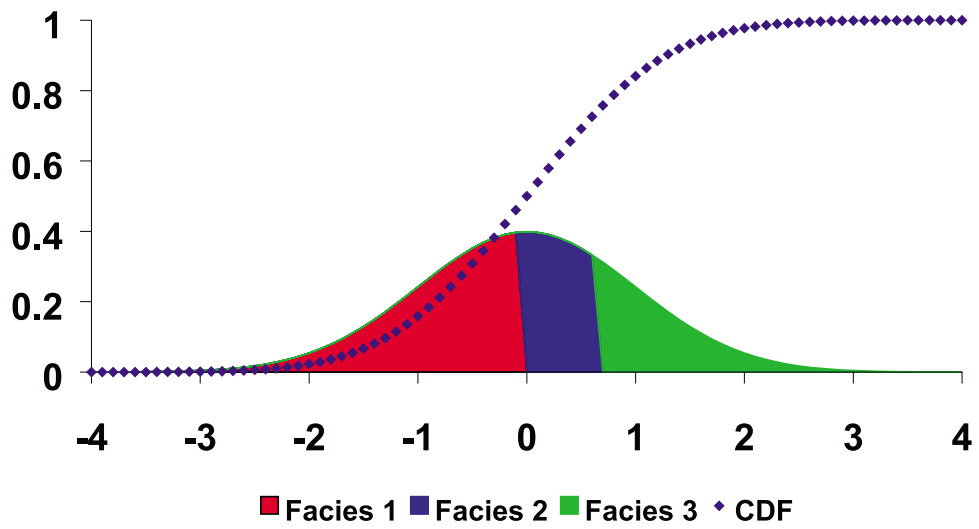


Figure 21: Normal score transformation of facies type.

Figure 22: Indicator variogram model left: vertical and right: horizontal variograms red: indicator and green normal score variogram.

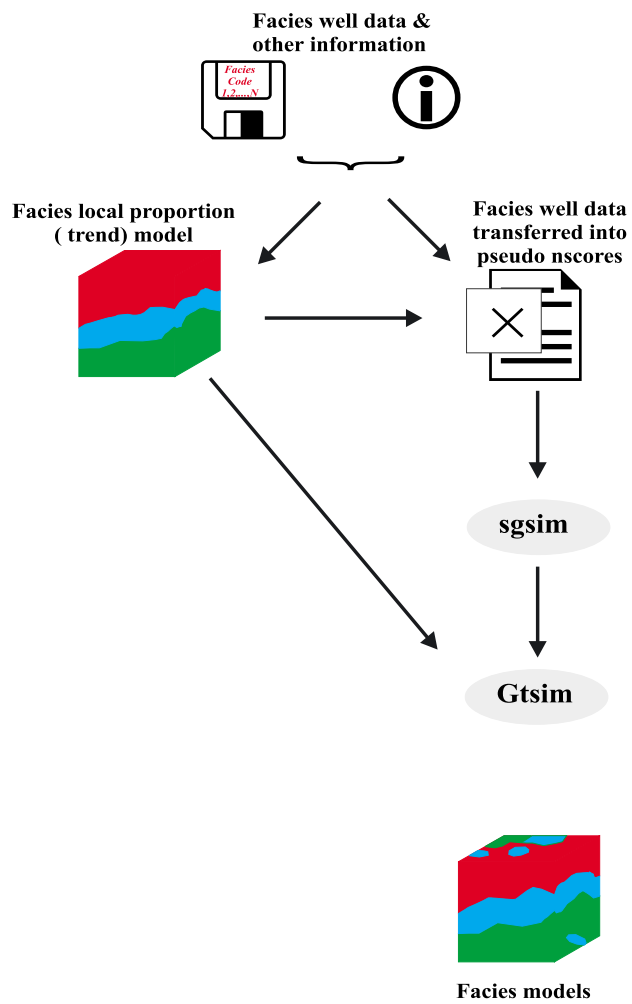


Figure 23: Procedure for facies modeling.

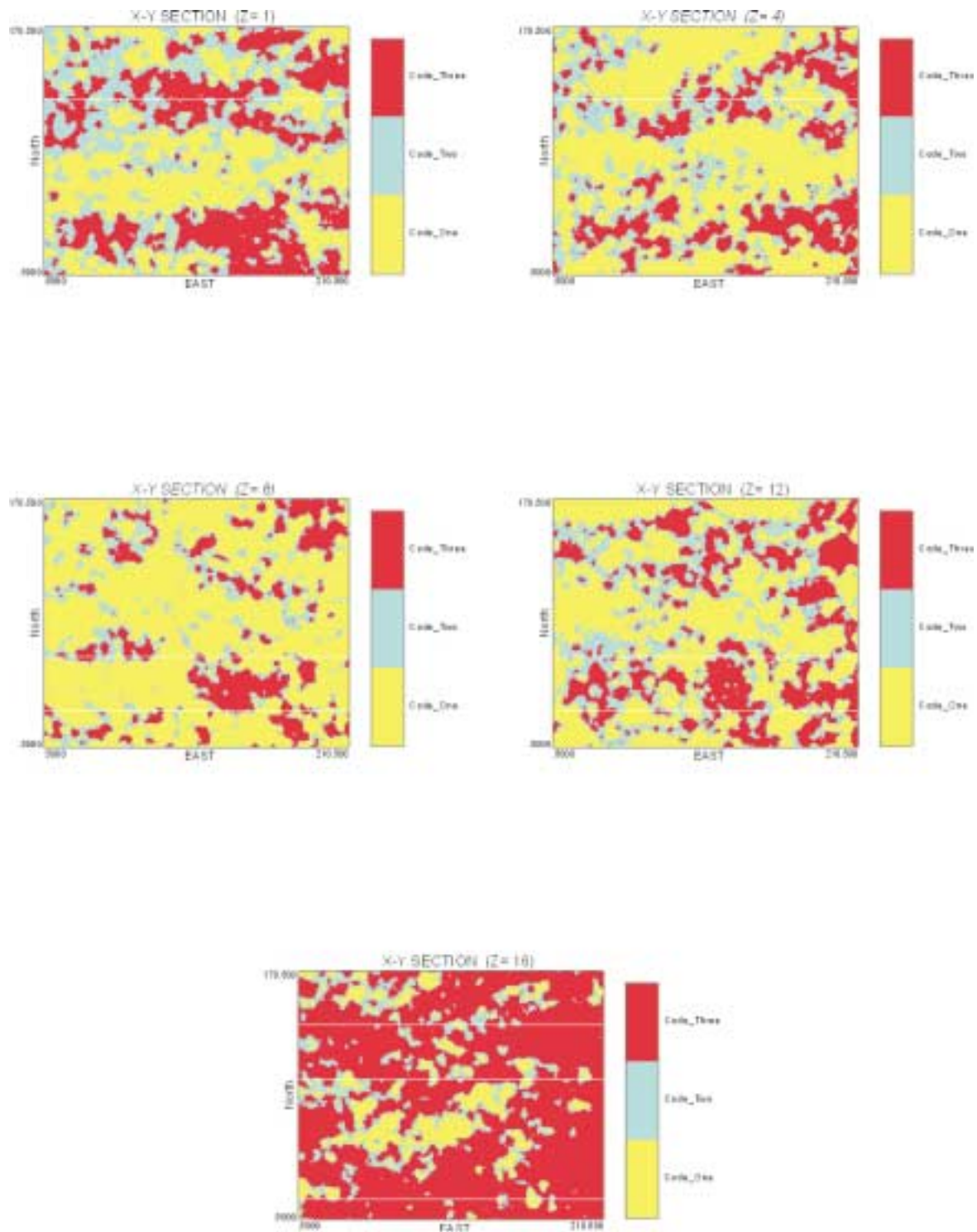


Figure 24: Plan view of facies model.

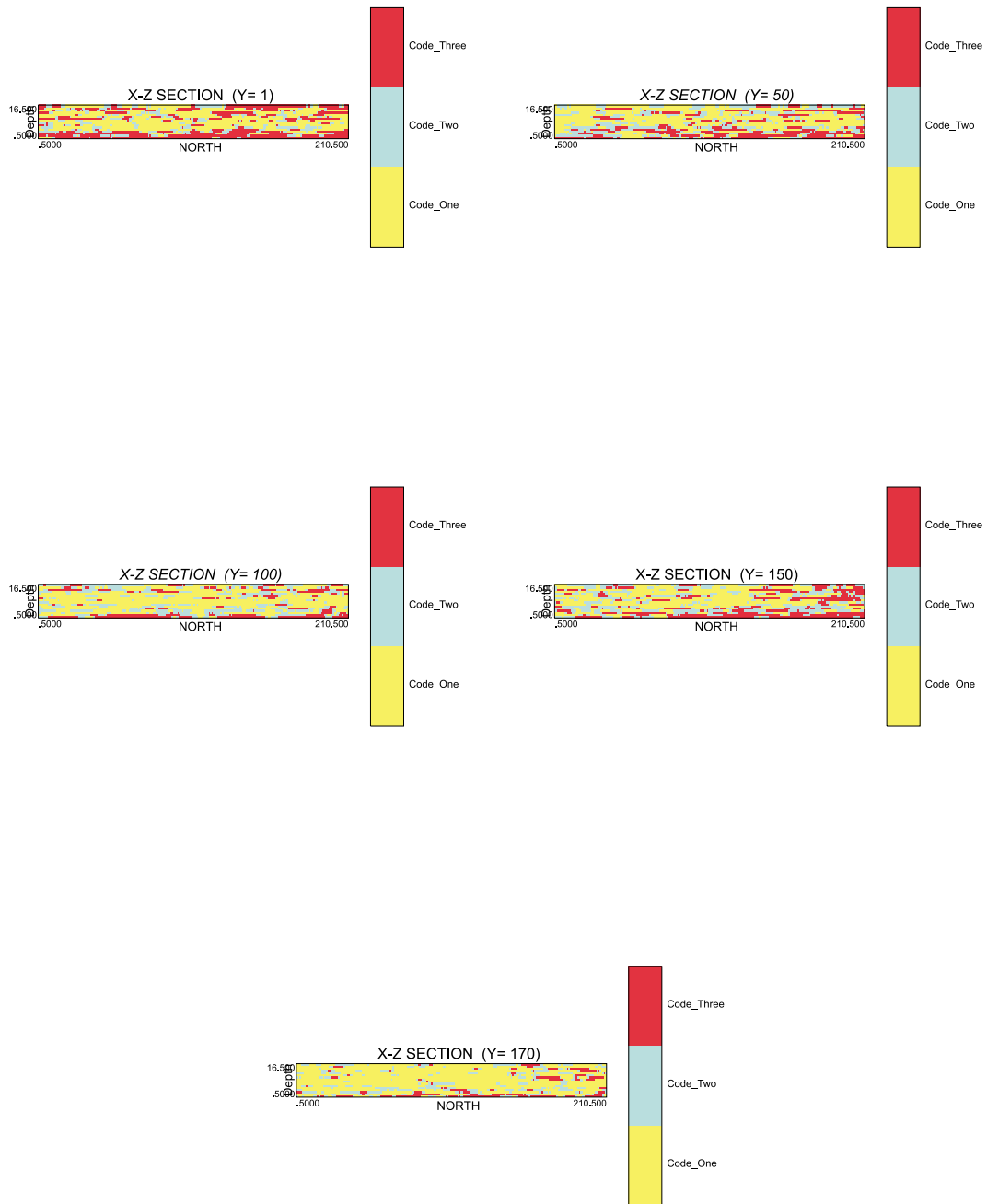


Figure 25: Cross section view along North-South direction.

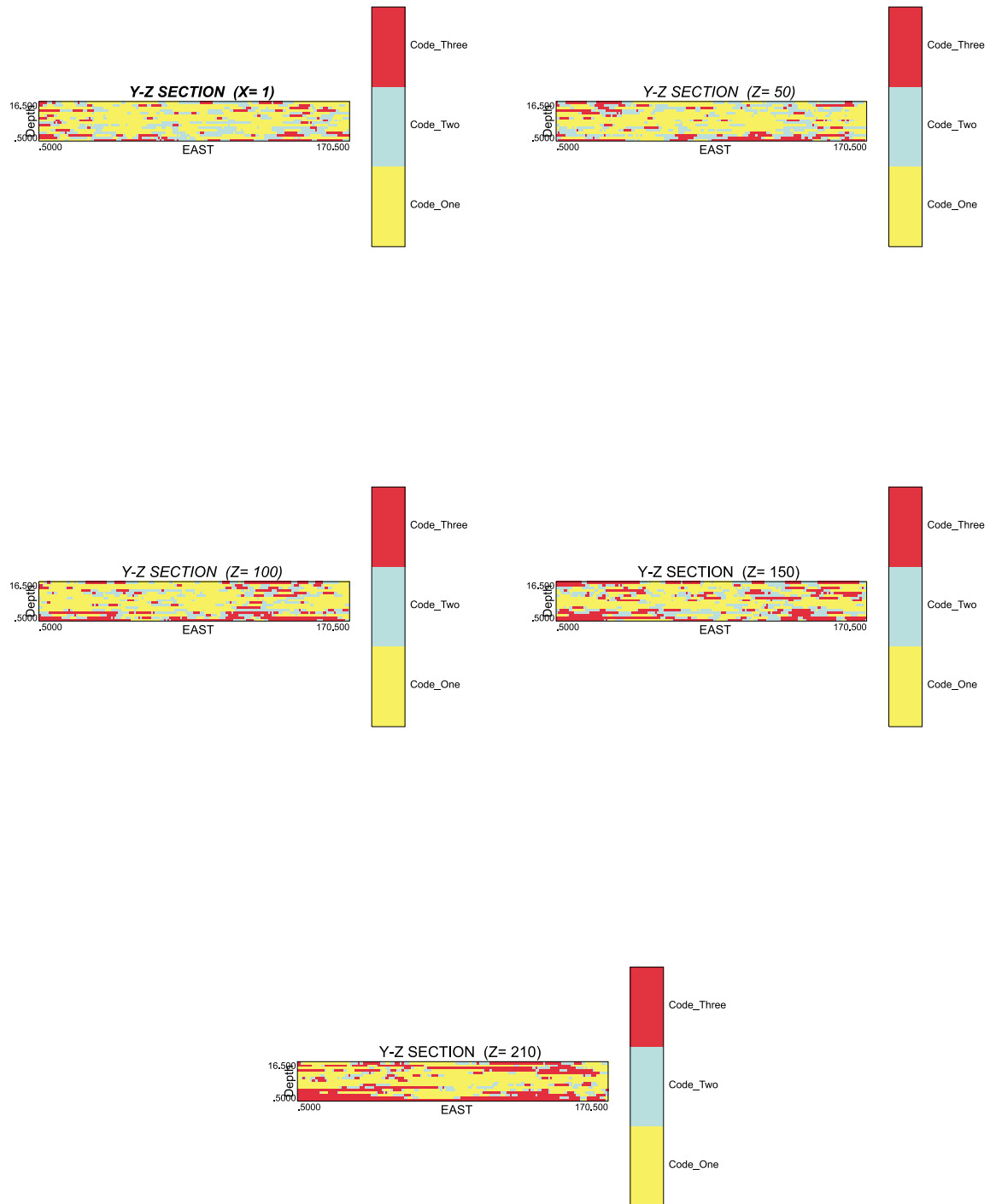


Figure 26: Cross section view along West-East direction.

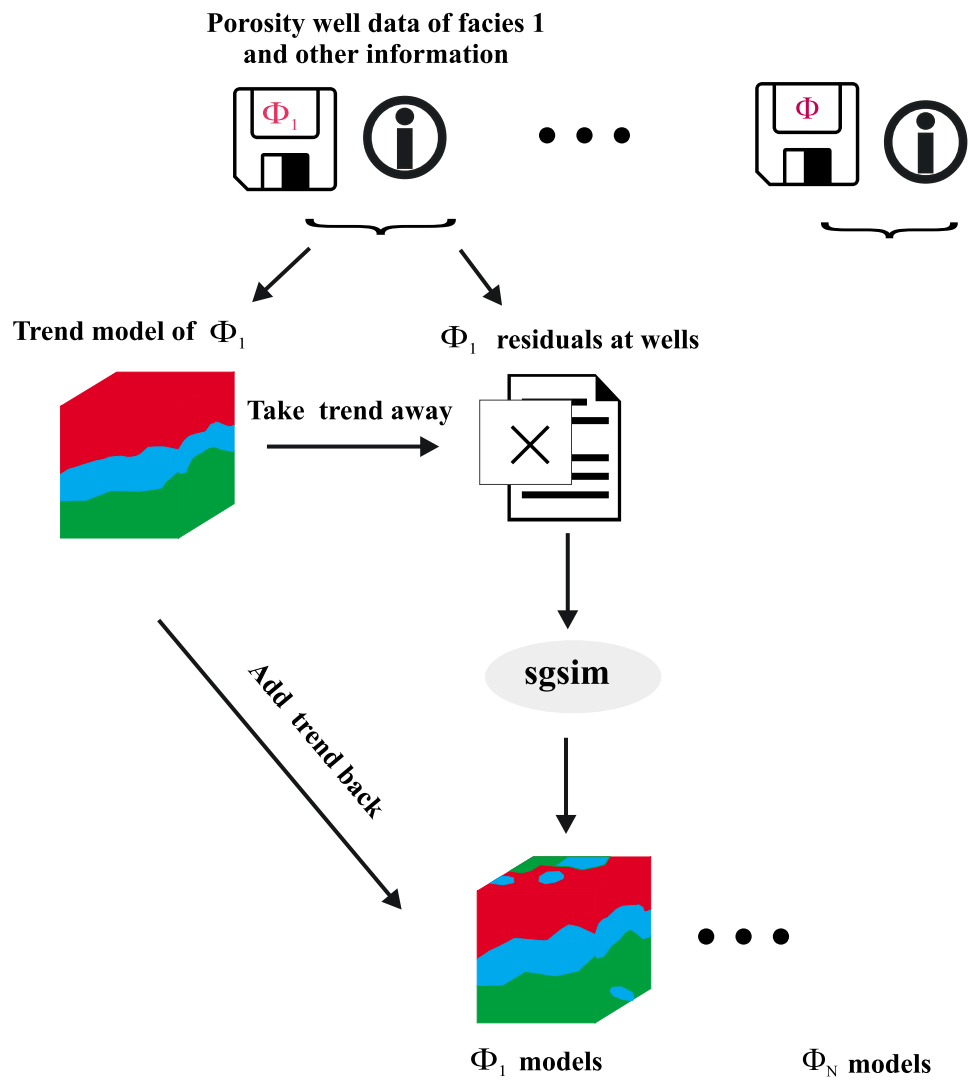


Figure 27: Procedure for porosity/permeability simulation.

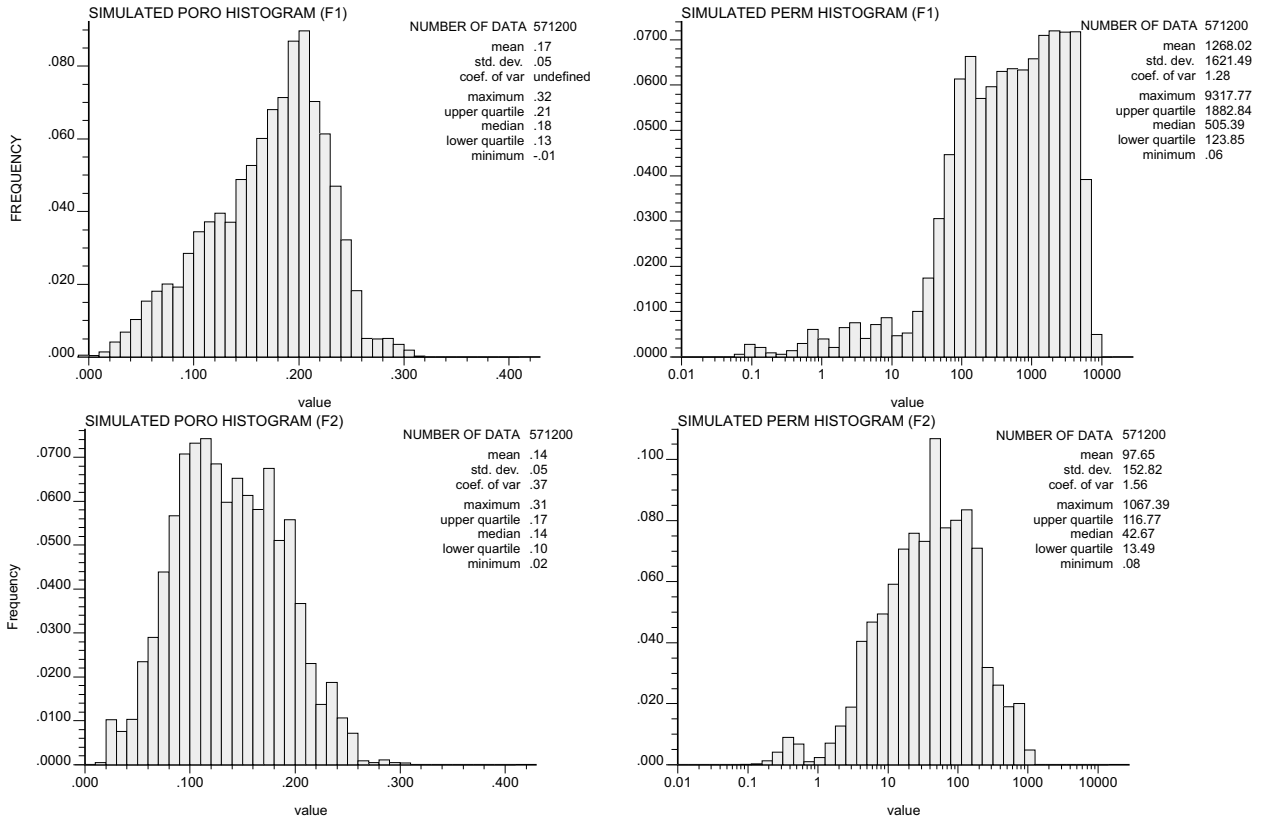


Figure 28: Histograms of porosity (left) and permeability (right) for facies 1(top) and facies 2 (bottom).

Parameters for d1interp

```

START OF PARAMETERS:
d1interp.out           - file output with the 2D interpolation
210 280050 100.48     - nx,xmn xsiz
3                      - number of variable
5                      - number of control points
280050 0.55 0.27 0.18 - x, value
285300 0.54 0.27 0.19 - x, value
290550 0.53 0.22 0.25 - x, value
295800 0.38 0.24 0.38 - x, value
301050 0.41 0.15 0.44 - x, value
  
```

Figure 29: Parameter file for **D1INTERP**.

Parameters for d3prop

```
START OF PARAMETERS:
d3prop.out           - output file of 2D trend from two 1D trends
210  280050  100.0   - nx, xmn, xsiz
170  1713050 100.0   - ny, ymn, ysiz
16   0.7716  1.5432  - nz, zmn, zsiz
3                                     - no. of facies
..\d1interp\d1interpx.out - input file of 1D trend in x direction
2,3,4                               - col
..\d1interp\d1interpy.out - input file of 1D trend in y direction
2,3,4                               - col
..\d1interp\d1interpz.out - input file of 1D trend in z direction
2,3,4                               - col
```

Figure 30: Parameter file for **D3PROP**.

Parameters for G2DTREND

```
START OF PARAMETERS:
trendeqn.for        - file with trend equations (FORTRAN)
g2dtrend.out        - file for final output models
210  280050  100.0   - nx,xmn,xsiz
170  1713050 100.0   - ny,ymn,ysiz
```

Note on the structure of the FORTRAN file :

```
C subroutine trendeqn(x,y,var)
C
C var is function of x and y
C var = f(x,y)
C return
C end
```

Figure 31: Parameter file for **G2DTREND**.

Parameters for GWLTREND

START OF PARAMETERS:

thickall.dat - data file with X, Y and variable
 1 2 5 - column no. for X, Y and variable
 trendeqn.for - file with trend equations (FORTRAN)
 gwltrend.out - file for final output models

Note on the structure of the FORTRAN file :

C subroutine trendeqn(x,y,var)
 C
 C var is function of x and y
 C var = f(x,y)
 C return
 C end

Figure 32: Parameter file for **GWLTREND**.

Parameters for GRETREND

START OF PARAMETERS:

kb2d_thk_rs.out - file with 2D residual data
 1 - column no. for residuals
 g2dtrend.out - file with trend data
 3 - column no. for trend
 gretrend.out - file for variables with trends added
 1 - number of realizations to generate
 210 280050 100.0 - nx,xmn,xsiz
 170 1713050 100.0 - ny,ymn,ysiz

Figure 33: Parameter file for **GRETREND**.

Parameters for GTSIM

START OF PARAMETERS:

sgsim.out - file with input Gaussian realizations
 gtsim.out - file for output categorical realizations
 1 - number of realizations
 210 170 16 - nx,ny,nz
 3 - number of categories
 1 0.25 - cat(1) global proportion(1)
 2 0.25 - cat(2) global proportion(2)
 3 0.50 - cat(3) global proportion(3)

```

1          - proportion curves (0=no, 1=yes)
facies1.dat - file with local proportion (1)
1          - column number for proportion
facies2.dat - file with local proportion (2)
2          - column number for proportion
facies3.dat - file with local proportion (3)
3          - column number for proportion

```

Figure 34: Parameter file for **GTSIM**.

```

Parameters for NSCOREF
*****

START OF PARAMETERS:
facies.dat          - file input with facies type
nscoref.out        - file output with nscore of facies
210  280050  100    - nx,xmn xsiz
170   1713050 100   - ny,ymn ysiz
16    0.7716  1.5432 - nz,zmn zsiz
1 2 4 5            - column for x,y,z,facies
3                  - number of facies
1   0.25           - global proportion f facies (1)
2   0.50           - global proportion f facies (2)
3   0.25           - global proportion f facies (3)
1                  - local proportion curves (0=no, 1=yes)
..\d3prop\d3prop.out - file with local proportion
4,5,6              - column for facies

```

Figure 35: Parameter file for **NSCOREF**.

```

Parameters for SGSIM
*****

START OF PARAMETERS:
Facies_Nscore.txt  - File With Data
 1  2  4  6  0  0  - Columns for X,Y,Z,vr,wt,sec.var.
-5  1E+21          - trimming limits
0                  - transform the Data (0=no, 1=yes)
sgsim.trn          - File for Output trans table
0                  - consider ref. dist (0=no, 1=yes)
histsmth.out       - File With ref. dist Distribution
 1  2              - Columns for vr and wt
-4  4              - zMin,zMax(Tail extrapolation)
 1  0              - lower Tail option, parameter
 1  4              - upper Tail option, parameter
 1                  - debugging level: 0,1,2,3

```

C:\Task\GTSIM\sgsim.dbg	- File for debugging Output
C:\Task\GTSIM\sgsim.out	- File for simulation Output
1	- number of Realizations to generate
210 280050 100	- nx,xmn,xsiz
170 1713050 100	- ny,ymn,ysiz
16 0.7716 1.5432	- nz,zmn,zsiz
69069	- random number seed
0 8	- Min and Max Original Data for sim
12	- number of simulated nodes to use
1	- assign Data to nodes (0=no, 1=yes)
1 3	- multiple grid search (0=no, 1=yes),num
0	- Maximum Data per octant (0=not used)
5000 5000 0.5	- Maximum search radii (hMax,hMin,vert)
0 0 0	- angles for search ellipsoid
51 51 11	- Size of Covariance lookup table
0 0.6 1	- kType: 0=SK,1=OK,2=LVM,3=EXDR,4=COLC
../data/ydata.dat	- File With LVM, EXDR, or COLC Variable
4	- Column for secondary Variable
2 0.01	- nst, nugget Effect
3 0.55 0 0 0	- it,cc,ang1,ang2,ang3
1000 1000 3	- a_hMax, a_hMin, a_vert
3 0.44 0 0 0	- it,cc,ang1,ang2,ang3
3000 3000 17	- a_hMax, a_hMin, a_vert

Figure 36: Parameter file for **SGSIM**.